DALTON
FULL PAPER

NMR and structural studies of gold(I) chloride adducts with bidentate 2-, 3- and 4-pyridyl phosphines

Susan J. Berners-Price,*[a] Richard J. Bowen,[a] Trevor W. Hambley[b] and Peter C. Healy[a]

[a] *School of Science, Griffith University, Nathan, Brisbane, Queensland 4111, Australia. E-mail: S.Berners-Price@sct.gu.edu.au*
[b] *Division of Inorganic Chemistry, School of Chemistry, University of Sydney, Sydney, NSW 2006, Australia*

Received 27th November 1998, Accepted 17th February 1999

The 1 : 2 adducts of gold(I) chloride with the diphosphine ligands, 1,2-bis(di-*n*-pyridylphosphino)ethane (d*n*pype) for $n = 2$, 3 and 4 have been synthesized and solution properties characterized by NMR spectroscopy, including variable temperature one dimensional $^{31}P\{^{1}H\}$ and 2D [^{31}P, ^{31}P] COSY experiments. The results show the 3-pyridyl (d3pype) and 4-pyridyl (d4pype) adducts to exist as bis-chelated monomeric $[Au(d3pype)_2]^+$ and $[Au(d4pype)_2]^+$ while the 2-pyridyl (d2pype) adduct forms an equilibrium mixture of monomeric $[Au(d2pype)_2]^+$, dimeric $[\{Au(d2pype)_2\}_2]^{2+}$ and possibly tetrameric $[\{Au(d2pype)_2\}_4]^{4+}$ species in which the d2pype ligands coordinate in both bridging and chelated modes *via* the phosphorus atoms. The relative percentages of the species present are dependent on both temperature and solvent. A single crystal X-ray structure determination of the 4-pyridyl adduct obtained from ethanol/hexane shows the complex to crystallize as $[Au(d4pype)_2H]Cl_2\cdot 6H_2O$ with monomeric cations and one of the 4-pyridyl rings likely to be protonated. Crystals of the 2-pyridyl complex obtained from methanol solution have been shown by crystal structure determination to be the dimer $[(d2pype)Au(\mu\text{-}d2pype)]_2Cl_2\cdot 14H_2O$, in which each gold atom is coordinated by one chelated and two bridging d2pype ligands. The solubility properties and solution behaviour of these three systems are compared to the analogous 1,2-bis(diphenylphosphino)ethane (dppe) system and the potential significance of these results to the antitumour properties of chelated 1 : 2 Au(I) diphosphine complexes are discussed.

The bis-chelated 1 : 2 Au(I) diphosphine complex $[Au(dppe)_2]Cl$ (where dppe is $Ph_2P(CH_2)_2PPh_2$) has been shown to exhibit antitumour activity against a range of tumour models in mice[1] and structure activity relationships have been evaluated for a wide range of diphosphine ligands and their metal complexes.[2–7] For complexes of the type $[Au(cis\text{-}R_2PCH{=}CHPR'_2)]^+$ and $[Au(R_2P(CH_2)_nPR'_2)_2]^+$ highest activity was found where R = R′ = phenyl and $n = 2$, 3.[5] In general, activity was reduced, or lost altogether when the phenyl substituents on the phosphine were replaced by other substituents, but retained when Au(I) was substituted by Ag(I) or Cu(I).[3,4] Although the mechanism for the cytotoxicity is not known, tumour cell mitochondria are likely targets for these large lipophilic cations[8,9] and, indeed, the complex $[Ag(eppe)_2]NO_3$ (where eppe is $Ph_2P(CH_2)_2PEt_2$) exhibits selective primary antimitochondrial activity in yeast.[10] However, a major difficulty in the clinical use of these compounds is that they target mitochondria in all cells, resulting in unacceptably high levels of toxicity.[11–13] Studies of the antitumour activity of other large lipophilic cations, such as bis quaternary ammonium heterocycles[14] and trialkylphosphonium salts,[15] have demonstrated a relationship between antitumour selectivity and lipophilic–hydrophilic balance. We have adopted the approach in our work on the antitumour properties of $[M(P\text{–}P)_2]^+$ cations of replacing the phenyl substituents of the diphosphine with pyridyl substituents in order to vary the hydrophilic character of the complexes while retaining the aromatic properties of the ligand substituent group.[16] We have recently reported improved methods for the synthesis of monodentate and bidentate pyridyl phosphines which allows synthesis of previously almost inaccessible 3- and 4-pyridyl phosphines in good yield.[17] Our work was stimulated by the curious earlier observation that whereas the 2-pyridyl analog had comparable antitumour activity in mice bearing P388 leukaemia to $[Au(dppe)_2]Cl$, the 4-pyridyl complex was inactive.[5] To rationalize these trends in activity, a detailed knowledge of the structural and solution chemistry of the complexes is required. Towards this goal, we have carried out a series of solution state NMR studies of the 1 : 2 complexes of gold(I) chloride with the diphosphine ligands 1,2-bis(di-*n*-pyridylphosphino)ethane (d*n*pype) for $n = 2$, 3, 4 and completed single crystal X-ray structure determinations on crystals of the 2- and 4-pyridyl complexes. These results show similar trends to those found in our recently reported study of the solid state and solution properties of 1 : 2 complexes of Ag(I) nitrate with these pyridyl diphosphine ligands.[18] The 3-pyridyl and 4-pyridyl complexes are monomeric $[Au(dnpype)_2]^+$ cations in solution and the 4-pyridyl complex crystallized as $[Au(d4pype)_2H]Cl_2\cdot 6H_2O$. In contrast the 2-pyridyl adduct crystallized as the dimeric complex $[(d2pype)Au(\mu\text{-}d2pype)]_2Cl_2\cdot 14H_2O$ and in solution forms equilibrium mixtures of monomeric $[Au(d2pype)_2]^+$, dimeric $[\{Au(d2pype)_2\}_2]^{2+}$ and possibly tetrameric $[\{Au(d2pype)_2\}_4]^{4+}$, with the relative percentages of the species present dependent on temperature and solvent.

Experimental

Preparation of compounds

The d*n*pype ligands for $n = 2$, 3 and 4 were prepared as described elsewhere.[17] $Na[AuCl_4]\cdot 2H_2O$ was purchased from Johnson Matthey, Au(CO)Cl was purchased from Strem Chemicals and $[NBu_4][AuCl_2]$ was prepared by the reduction of $[NBu_4][AuCl_4]$ with sodium acetylacetonate, as described elsewhere.[19]

$[(AuCl)_2(d2pype)]$. (a) $Na[AuCl_4]\cdot 2H_2O$ (0.36 g, 0.91 mmol) was reduced to Au(I) by thiodiglycol (0.43 g, 3.5 mmol) in

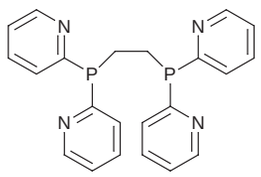

d2pype

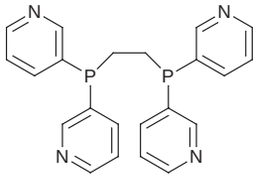

d3pype

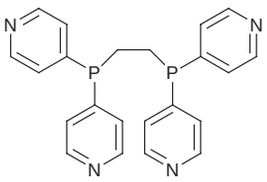

d4pype

aqueous acetone (3:1, 4 cm^3) cooled to between 0 and 5 °C. When the solution became colourless it was added dropwise to a suspension of d2pype (0.20 g, 0.50 mmol) in acetone (40 cm^3). The volume of the solvent was concentrated to *ca.* 20 cm^3 and cooled overnight at −20 °C to yield a fine white crystalline material. This was recrystallized from 1:1 choroform/hexane and isolated by filtration (yield 0.26 g, 60%), mp 293–295 °C (lit.[2] 292–293 °C) (Found: C, 30.1; H, 2.3; N, 6.2. $C_{22}H_{20}Au_2N_4P_2Cl_2$ requires: C, 30.5; H, 2.3; N, 6.5%).

(b) $[NBu_4][AuCl_2]$ (0.250 g, 0.50 mmol) and d2pype (0.101 g, 0.25 mmol) were suspended in 5 ml of dimethylformamide. Stirring the solution for 10 minutes resulted in dissolution of the starting materials and precipitation of the complex as a fine white crystalline powder which was isolated by filtration (yield 0.13 g, 60%), mp 293–295 °C.

[(AuCl)$_2$(d3pype)]. $[NBu_4][AuCl_2]$ (1.015 g, 1.99 mmol) was added to a stirred solution of d3pype (0.40 g, 0.99 mmol) in CH_2Cl_2 (25 cm^3) resulting in a clear yellow solution from which a fine white precipitate formed after a few minutes. After further stirring for 4 hours the flask was cooled overnight at −20 °C and the product isolated by filtration. Yield, 0.60 g, 69%, mp 222–229 °C (decomp.) (Found: C, 30.1; H, 2.5; N, 6.5. $C_{22}H_{20}Au_2N_4P_2Cl_2$ requires: C, 30.5; H, 2.3; N, 6.5%).

[(AuCl)$_2$(d4pype)]. The compound $[NBu_4][AuCl_2]$ (0.254 g, 0.50 mmol) was added as a solid to a stirred solution of d4pype (0.10 g, 0.25 mmol) in CH_2Cl_2 (25 cm^3) resulting in precipitation of the complex as a white crystalline powder isolated by filtration. Yield 0.15 g, 69%, mp 234–244 °C (lit.[2] 241–242 °C) (Found: C, 30.3; H, 2.25; N, 6.5. $C_{22}H_{20}Au_2N_4P_2Cl_2$ requires: C, 30.5; H, 2.3; N, 6.5%).

[Au(d2pype)$_2$]Cl·7H$_2$O. $Na[AuCl_4]\cdot 2H_2O$ (0.18 g, 0.45 mmol) was reduced to Au(I) by thiodiglycol (0.23 g, 1.9 mmol) in aqueous acetone (3:1, 4 cm^3) cooled to *ca.* 0 °C. When the solution became colourless it was added dropwise to a suspension of d2pype (0.40 g, 0.99 mmol) in acetone (60 cm^3). A clear yellow solution resulted and after stirring this solution for 5 min at room temperature, a yellow solid precipitated. After further stirring for 1 h the solid was collected by filtration and recrystallized from ethanol/hexane. Yield 0.41 g, 70%, mp 254–255 °C (lit.[5] 257–258 °C) (Found: C, 45.2; H, 4.3; N, 9.45. $C_{44}H_{54}AuN_8O_7P_4Cl$ requires: C, 45.4; H, 4.7; N, 9.6%). Crystals of the water solvated dimer, $[Au(d2pype)_2]_2Cl_2\cdot nH_2O$, of marginal suitability for X-ray structure determination, were obtained by recrystallization from methanol.

[Au(d3pype)$_2$]Cl·6H$_2$O·(CH$_3$)$_2$SO. $[NBu_4][AuCl_2]$ (0.236 g, 0.46 mmol) was added as a solid to a stirred solution of d3pype (0.40 g, 0.99 mmol) in dmso (20 cm^3) under an atmosphere of argon. The resulting clear yellow solution was stirred overnight, then Et_2O (10 cm^3) was added. After refrigeration for several hours the solution settled into two layers. The complex was afforded as a yellow solid on addition of toluene (30 cm^3) and cooling for 24 h at −20 °C (yield 0.32 g, 56%), mp 234–242 °C (Found: C, 44.9; H, 4.1; N, 9.1. $C_{46}H_{58}N_8P_4O_7SAuCl$ requires: C, 45.2; H, 4.8; N, 9.2%). The presence of six solvated water molecules and a dmso molecule in the crystal lattice was confirmed from a ^{1}H NMR spectrum in dmf-d$_7$.

Table 1 ^{31}P NMR Parameters for $[(AuCl)_2(dn\text{pype})]$ and $\{[Au(dn\text{pype})_2]^+\}_n$ complexes[a]

Compound	Solvent	T/K	$\delta\,^{31}P$[a] P_A	P_B	P_C
$[(AuCl)_2(d2pype)]$	dmf	295	31.0		
$[(AuCl)_2(d3pype)]$	dmso	295	23.2		
$[(AuCl)_2(d4pype)]$	dmf	295	29.7		
$\{[Au(d2pype)_2]Cl\}_n$	CD_3OD				
$n = 1$		293	26.8		
$n = 2$			18.8	25.3	
$n = 4$[b]		213	15.3	18.0	25.5
$[Au(d3pype)_2]Cl$	CD_3OD	298	13.1		
$[Au(d4pype)_2]Cl$	CD_3OD		21.1		

[a] Referenced to external 85% H_3PO_4 at 295 K. [b] Tentative assignment, see text.

[Au(d4pype)$_2$]Cl·4H$_2$O. (a) The compound d4pype (0.40 g, 1.0 mmol) was added as solid to a stirred slurry of Au(CO)Cl (0.13 g, 0.50 mmol) in dry, degassed thf (20 cm^3) in a flame-dried argon filled Schlenk flask, resulting in the immediate formation of a white precipitate. The solid was collected by filtration, dissolved in methanol and insoluble material filtered off. The compound precipitated as a white solid on addition of Et_2O to the filtrate (yield 0.43 g, 78%), mp 294–296 °C (lit.[5] 291–293 °C) (Found: C, 47.7; H, 4.3; N, 9.9. $C_{44}H_{48}Au_{48}N_8O_4P_4Cl$ requires: C, 47.6; H, 4.4; N, 10.1%).

(b) $Na[AuCl_4]\cdot 2H_2O$ (0.10 g, 0.25 mmol) was reduced to Au(I) by thiodiglycol (0.07 g, 0.57 mmol) in aqueous acetone (3:1, 4 cm^3) cooled to *ca.* 0 °C. When the solution became colourless it was added dropwise to a solution of d4pype (0.22 g, 0.55 mmol) in 1:1 acetone:methanol (50 cm^3) to give a clear yellow solution. The solvent was removed by rotary evaporation to give a yellow oil. The compound precipitated on addition of acetone. Small crystals of $[Au(d4pype)_2H]Cl_2\cdot 6H_2O$, of marginal quality for X-ray structure determination, were obtained by recrystallization from ethanol/hexane after 6 weeks storage at −20 °C.

NMR Spectroscopy

^{1}H, ^{13}C and ^{31}P NMR spectra were recorded on either Varian Gemini-200 or UNITY-400 spectrometers and were referenced as indicated in Tables 1–3. Typically, $^{31}P\{^1H\}$ spectra were recorded with a pulse angle of 45° and a relaxation delay of 1 s. Two dimensional phase-sensitive ^{31}P homonuclear shift correlated (COSY) spectra were recorded with WALTZ-16 modulated ^{1}H decoupling. The spectral width in F2 was 4864 Hz with 2048 data points. A total of 128 FID's were taken in F1 with 88 scans each. The recycle delay was set to 3 s to give a total experiment time of 7 hours. NMR data for the complexes are shown in Tables 1–3 and spectra presented in Figs. 1–5.

Crystallography

X-Ray data collections were performed at 294 K using an Enraf-Nonius CAD4-F diffractometer with Mo-K_α radiation and scintillation counter for $[Au(d4pype)_2H]Cl_2\cdot 6H_2O$ and a Rigaku AFC7-R four-circle diffractometer (rotating anode

Table 2 ^{13}C NMR data for 2-, 3- and 4-pyridyl ligands and Au(I) complexes (at ambient temperature)[a]

Compound	Solvent	$\delta\ ^{13}C$[b] (J (C, P)/Hz)					
		C_2	C_3	C_4	C_5	C_6	CH_2
d2pype[c]	$CDCl_3$	162.3	129.1 vt (11)	136.3	123.0	149.8	22.1
$\{[Au(d2pype)_2]Cl\}_n$[d]	CD_3OD	157.8	130.2	138.9	126.2	151.3	27.5
d3pype	$CDCl_3$	153.2 vt (12.6)	132.4 vt (9.0)	139.8 vt (7.3)	123.7	150.3	22.9
$[(AuCl)_2(d3pype)]$	dmso	153.3 vt (7.6)	124.8 vt (29)	141.1 vt (6.1)	124.2	152.8	21.0
$[Au(d3pype)_2]Cl$	CD_3OD	151.9	127.7	141.4	125.8	151.9	27.2
d4pype	$CDCl_3$	149.8	126.9 vt (8.1)	146.3 vt (9.9)	126.9 vt (8.1)	149.8	22.3
	CD_3OD	150.2	128.9 vt (8.5)	nr[e]	128.9 vt (8.5)	150.2	23.2
$[(AuCl)_2(d4pype)]$	dmf	151.2	128.3	138.8	128.3	151.2	21.1
$[Au(d4pype)_2]Cl$	CD_3OD	151.3	127.8	142.5	127.8	151.3	27.5

[a] Referenced to TMS. [b] Singlet, unless otherwise stated. [c] Assignments based on ^{13}C assignments for the bidentate 2-pyridylphenylphosphine $Ph(2\text{-py})P(CH_2)_2PPh(2\text{-py})$.[33] [d] Separate ^{13}C resonances for monomer ($n = 1$) and dimer ($n = 2$) are not resolved. [e] nr = Not resolved.

Table 3 ^1H NMR data for 2-, 3- and 4-pyridyl ligands and Au(I) complexes (at ambient temperature)[a]

Compound	Solvent	$\delta\ ^1H$					
		H_2	H_3	H_4	H_5	H_6	CH_2[b]
d2pype	CD_3OD		7.43	7.69	7.29	8.56	2.44 (8.7)
$[(AuCl)_2(d2pype)]$	$CDCl_3$		7.78	7.94	7.38	8.74	3.15
$\{[Au(d2pype)_2]Cl\}_n$	CD_3OD						
$n = 1$			7.51	7.69	7.43	8.60	3.08
$n = 2$			7.36	7.53	7.29	8.34	3.08
			7.60	7.60	7.20	8.17	3.32
d3pype	$CDCl_3$	8.59		7.59	7.27	8.59	2.16 (8.7)
	D_2O	8.09		7.18	6.90	8.09	1.81
$[Au(d3pype)_2]Cl$	CD_3OD	8.61		7.83	7.39	8.61	2.91
$[(AuCl)_2(d3pype)]$	dmso-d_6	8.97		8.19	7.54	8.74	3.21[c]
d4pype	$CDCl_3$	8.58	7.18		7.18	8.58	2.12 (9.3)
	CD_3OD	8.39	7.27		7.27	8.39	2.19 (9.7)
$[(AuCl)_2(d4pype)]$	dmf-d_7	8.80	7.90		7.90	8.80	3.45
$[Au(d4pype)_2]Cl$	CD_3OD	8.51	7.32		7.32	8.51	2.91

[a] Referenced to either TMS or TSP (for solutions in D_2O). [b] Broad singlet or quasi-triplet ($J = [^2J(^{31}P–^1H) + {}^3J(^{31}P–^1H)]$ (Hz) in parentheses where resolved). [c] Tentative assignment due to overlap with solvent peak.

source) with Cu-K_α radiation and scintillation counter for $[Au(d2pype)_2]_2Cl_2\cdot 14H_2O$. The structures were solved by direct methods, extended by Fourier methods and refined by full matrix least squares refinement on $|F|$ for observed data N_o ($I > 2.5\sigma(I)$) after absorption corrections. Anisotropic thermal parameters were refined for all non-hydrogen atoms except the carbon atoms of the 4-pyridyl complex; (x, y, z, $U_{iso})_H$ were included, constrained at estimated values. Hydrogen atoms were not located on the solvent water molecules or protonated pyridine rings. The pyridyl nitrogen atoms in the 2-pyridyl complex were assigned on the basis of slightly shorter C–N bonds in all cases. However, the marginal quality of the structure determination makes this assignment tentative and the alternative assignment, or 50% C/N occupancy of the two sites, equally likely. The results for the 2-pyridyl complex also showed evidence for disorder in the peripheral carbon atoms of the pyridyl rings. Computation used teXsan[20] software and associated programs. Bond length and angle data are shown in Tables 4 and 5 and representative views of the molecules are given in Figs. 6 and 7.

Crystal/refinement data

$[Au(d4pype)_2H]Cl_2\cdot 6H_2O \equiv C_{44}H_{53}AuCl_2N_8O_6P_4$, $M = 1181.7$, monoclinic, space group $P2_1$ (C_2^2 No. 4), $a = 12.29(2)$, $b = 13.49(3)$, $c = 15.00(1)$ Å, $\beta = 95.1(1)°$, $U = 2477$ Å^3, $Z = 2$, $D_c = 1.58$ g cm^{-3}, $F(000) = 1188$, μ(Mo-K_α, $\lambda = 0.71069$ Å) = 32.1 cm^{-1}; crystal size = 0.13 × 0.20 × 0.17 mm; $T = 294$ K, $T_{min,max} = 0.63$, 0.72; $2\theta_{max} = 45°$, $N = 3550$, N_o ($I > 2.5\sigma(I)$) = 2617, R (on $|F|$) = 0.078, R_w ($w = 1/(\sigma^2F_o)$) = 0.090.

$[Au(d2pype)_2]_2Cl_2\cdot 14H_2O \equiv C_{88}H_{108}Au_2Cl_2N_{16}O_{14}P_8$, M = 2326.6, orthorhombic, space group $Pbcn$ (D_{2h}^{14} No. 60), a = 22.519(5), $b = 17.937(6)$, $c = 26.565(7)$ Å, $U = 10730$ Å^3, Z = 4, $D_c = 1.44$ g cm^{-3}, $F(000) = 4688$, μ(Cu-K_α, $\lambda = 1.5418$ Å) = 69.3 cm^{-1}; crystal size = 0.18 × 0.12 × 0.04 mm; $T = 294$ K, $T_{min,max} = 0.61$, 0.99; $2\theta_{max} = 120°$, $N = 8730$, N_o ($I > 2.5\ \sigma(I)$) = 3411, R (on $|F|$) = 0.070, R_w ($w = 1/(\sigma^2F_o)$) = 0.086.

CCDC reference number 186/1360.

See http://www.rsc.org/suppdata/dt/1999/1337/ for crystallographic files in .cif format.

Results and discussion

Synthesis of compounds

The 2:1 bridged di-gold complexes $[(AuCl)_2(dnpype)]$ were

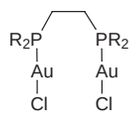

prepared either by the method described previously for $[(AuCl)_2(dppe)]$,[21] by the addition of 0.5 mol equivalent of the appropriate ligand to a solution of $Na[AuCl_4]$ that has been reduced to Au(I) *in situ* by reaction of Au(III) with thiodiglycol, or more conveniently by direct reaction of stoichiometric quantities of the ligand and the Au(I) salt, $[NBu_4][AuCl_2]$ according to the reaction below:

$$2[NBu_4][AuCl_2] + dn\text{pype} \longrightarrow [(AuCl)_2(dn\text{pype})] + 2[NBu_4]Cl \quad (1)$$

This reaction is particularly attractive because $[NBu_4][AuCl_2]$ is an anhydrous, easily prepared air stable salt[19] with the by-product from the reaction, $[NBu_4]Cl$, highly soluble in most organic solvents while the limited solubility of the neutral bridged di-gold compounds in these solvents is such that they precipitate readily and can be isolated by simple filtration.

The bis-chelated complex $[Au(dppe)_2]Cl$ is conveniently prepared in the solid state by addition of 2 mol equivalents of dppe to solution of Au(I) prepared *in situ* by reaction of Au(III) with thiodiglycol, the complex precipitating from solution due to its low solubility in water.[21] However, isolation of pure $[Au(dnpype)_2]Cl$ complexes by this method was found to be much less convenient because of difficulties encountered in separating these water soluble complexes and the thiodiglycol oxidation products. These complexes are better prepared by reaction with previously prepared anhydrous gold(I) salts, for example in the present studies, by addition of stoichiometric quantities of the d*n*pype ligand to the di-gold bridged complexes, $[(AuCl)_2(dnpype)]$, the carbonyl complex [Au(CO)Cl] or the $[NBu_4][AuCl_2]$ salt in an appropriate organic solvent.

All three 1:2 Au:d*n*pype adducts are soluble in dmso and methanol, but whereas both $[Au(d3pype)_2]Cl$ and $[Au(d4pype)_2]Cl$ are soluble in water and insoluble in CH_2Cl_2, the reverse trend is found for the 2-pyridyl complex which is soluble in CH_2Cl_2 and not significantly soluble in water.

NMR spectroscopy

We have shown from previous work on the dppe complexes that the formation of stable bis-chelated $[Au(P–P)_2]^+$ complexes in the solution state can be conveniently monitored by ^{31}P NMR titration of the bridged di-gold complex $[(AuCl)_2(P–P)]$ with free ligand (P–P).[21,22] With the aim of investigating the formation of the four-coordinate complexes, $[Au(dnpype)_2]Cl$, similar titrations were completed as part of the present work. For the 4-pyridyl system (Fig. 1), the spectrum of $[(AuCl)_2(d4pype)]$ consisted of a single resonance at δ 29.7. With addition of 0.5 mol. equivalents of d4pype this peak broadened and shifted to slightly lower frequency (δ 29.0) and a new broad peak appeared at δ 20.4. With further addition of d4pype the peak at δ 29.0 broadened further and decreased in intensity, while the peak at δ 20.4 increased in intensity and sharpened with each addition until the Au:d4pype ratio was greater than 1:2, when a peak for free d4pype (δ −15.4) appeared. Both peaks remained sharp showing a slow rate of ligand exchange on the NMR time scale. This behaviour is analogous to that observed previously for the bridged di-gold complex $[(AuCl)_2(dppe)]$ on titration with dppe,[21,22] in which the tetrahedral cation $[Au(dppe)_2]^+$ is formed on addition of dppe:

$$[(AuCl)_2(dppe)] + 3dppe \rightleftharpoons 2[Au(dppe)_2]Cl \quad (2)$$

The bis-chelated four-coordinate species was present in solution on addition of less than stoichiometric amounts of dppe and exchange of free and bound ligand occurred at a rate of $\ll 800\ s^{-1}$ at room temperature, demonstrating much enhanced thermodynamic and kinetic stability compared to that of $[Au(PR_3)_4]^+$ complexes containing monodentate phosphines. Similar behaviour was found for other $[Au(P–P)_2]^+$ complexes with five or six-membered chelate rings.[21]

By comparison with these results, the peak at δ 20.4 is assigned to the four-coordinate bis-chelated complex ion $[Au(d4pype)_2]^+$.

The titration of $[(AuCl)_2(d3pype)]$ (δ 23.2) with d3pype in dmso-d_6 at 295 K showed similar behaviour with evidence for the formation of $[Au(d3pype)_2]^+$ (δ 13.5), in slow exchange with free d3pype (δ −24.4) at Au:d3pype ratios greater than 1:2.

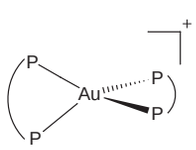

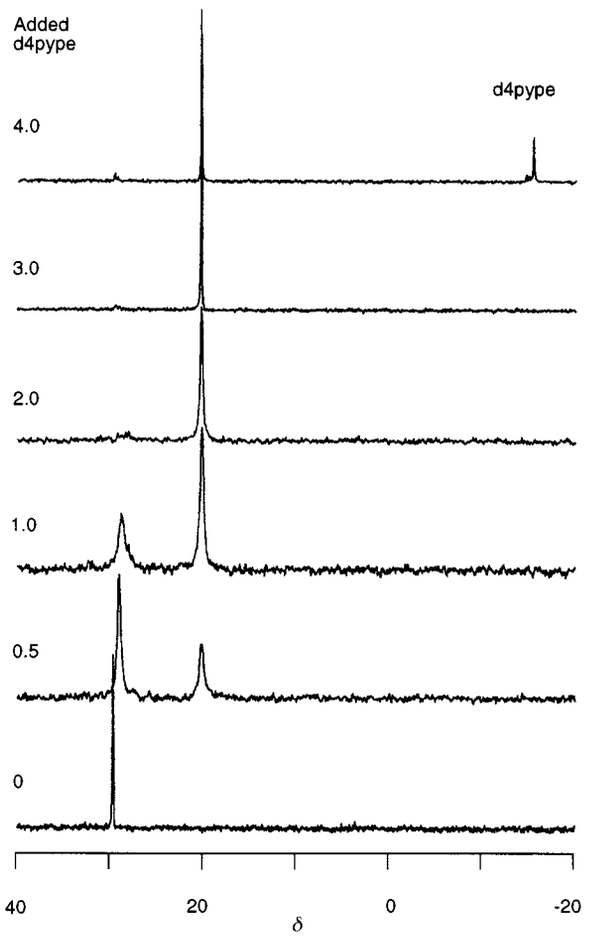

Fig. 1 161.9 MHz $^{31}P\{^1H\}$ NMR spectra at 295 K of 5.8 mM $[(AuCl)_2(d4pype)]$ in dmf in the presence of 0, 0.5, 1, 2, 3 and 4 mol equivalents of d4pype. In the top spectrum there are peaks assignable to a small amount of d4pype-mono-oxide (δ 29.4, −14.7, $^3J(^{31}P–^{31}P) = 53$ Hz) in addition to $[Au(d4pype)_2]^+$ (δ 20.4) and d4pype (δ −15.4).

Formation of bis-chelated monomeric $[Au(dnpype)_2]^+$ cations is confirmed also by the ^1H and ^{13}C NMR spectra of the 1:2 adducts of Au(I) with d3pype and d4pype (Tables 2 and 3). For bidentate phosphines with $(CH_2)_2$ backbones the CH_2 protons constitute the AA′ part of an $A_2XX'A'_2$ spin system as a result of unequal $^{31}P–^1H$ spin–spin coupling to the two P atoms and give rise to a quasi-triplet in which the separation of the outer two peaks corresponds approximately to $[^2J(^{31}P–^1H) + {}^3J(^{31}P–^1H)]$.[23] This pattern is observed for the d*n*pype ligands (Table 3) and the small coordination shift to higher frequency ($\Delta\delta$ +0.7–1.1) and broadening of the $(CH_2)_2$ resonance to give an unresolved multiplet is characteristic of the behaviour observed previously for bis-chelated gold(I) diphosphine complexes[21] and also for the analogous 1:2 Ag(I) d3pype and d4pype complexes.[18] These $(CH_2)_2$ protons are significantly less shielded (by 0.3–0.5 ppm) than those in the bridged di-gold complexes. For $[Au(dppe)_2]Cl$ the aromatic protons were shielded with respect to those of the free diphosphine but, as found for $[Ag(dnpype)_2]NO_3$ ($n = 3$, 4), this was not observed for the bis-chelated Au(I) 3- and 4-pyridyl complexes where all aromatic protons are slightly deshielded with respect to the free ligands (Table 3).

In contrast to the above results, titration of a solution of $[(AuCl)_2(d2pype)]$ with the free d2pype ligand in dmf showed a slightly different pattern of behaviour (Fig. 2). With the addition of 0.5 eq of d2pype the ^{31}P resonance for $[(AuCl)_2(d2pype)]$ at δ 31.0 decreased in intensity and a new peak

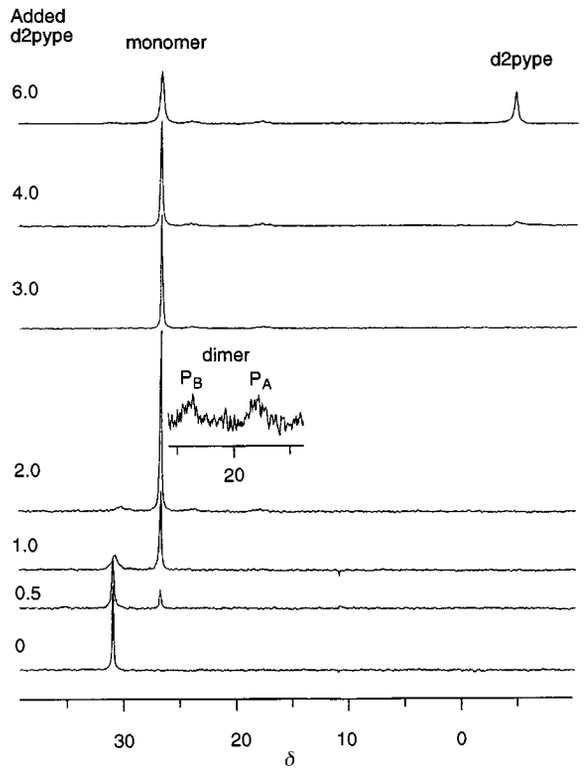

Fig. 2 81.0 MHz $^{31}P\{^1H\}$ NMR spectra at 295 K of 6 mM $[(AuCl)_2(d2pype)]$ in dmf in the presence of 0, 0.5, 1, 2, 3, 4 and 6 equivalents of d2pype.

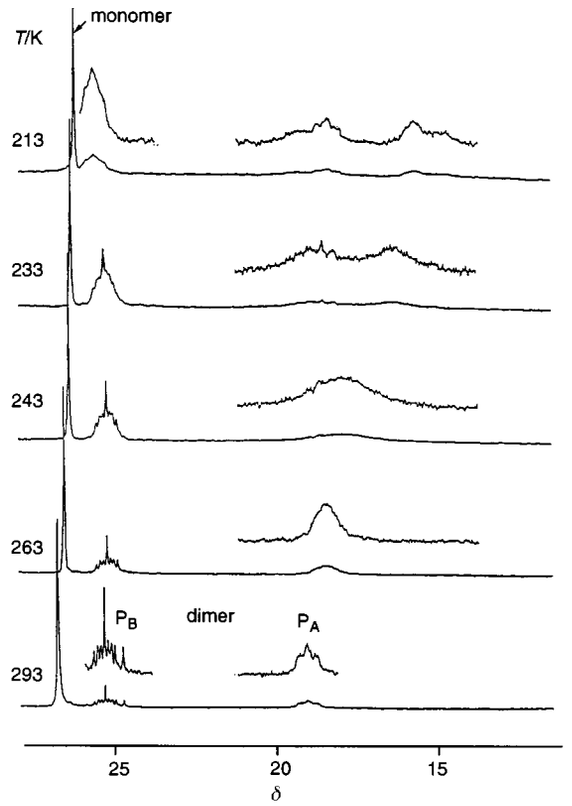

Fig. 3 161.9 MHz $^{31}P\{^1H\}$ NMR spectra of $\{[Au(d2pype)_2]Cl\}_n$ in CH_3OH–30% CH_3OD at 293, 263, 243 and 233 and 213 K. The resonances at 293 K are assigned to the monomeric and dimeric species $\{[Au(d2pype)_2]^+\}_n$. A minor peak (not shown) representing *ca.* 4% of the total Au–P species is also observed at δ 31.4. On cooling this peak broadened and disappeared below 253 K. Although unassigned its chemical shift is similar to $[(AuCl)_2(d2pype)]$ (Fig. 1).

appeared at δ 26.8. The latter peak increased in intensity with further addition of d2pype and reached a maximum intensity at a Au : d2pype ratio of 1 : 2. At higher Au : d2pype ratios a peak for free d2pype (δ −4.5) was resolved, in slow exchange on the NMR time scale with the δ 26.8 resonance. The species at δ 26.8 is assignable to the monomeric bis-chelated complex $[Au(d2pype)_2]^+$. However, at Au : d2pype ratios >2 : 3 two minor broadened multiplets at δ 24.2 and δ 17.9 were also resolved in the ^{31}P spectra (Fig. 2). For the analogous Ag(I) system, we have shown previously from ^{31}P and ^{109}Ag NMR studies that a temperature and solvent dependent equilibrium occurs between monomeric, dimeric and trimeric forms of the 1 : 2 Ag(I) : d2pype complexes.[18] To investigate whether similar equilibria occur for the Au(I) system we carried out variable temperature ^{31}P NMR studies for a sample of the 1 : 2 Au(I) : d2pype adduct in different solvents. Curiously, in dmf only the singlet at δ 26.8 attributable to monomeric $[Au(d2pype)_2]^+$ was observed and the multiplets at δ 24.2 and δ 17.9 were not observed on lowering the temperature, although this had been observed as a minor species on titration of $[(AuCl)_2(d2pype)]$ with d2pype in this solvent. Similarly, in CD_2Cl_2 only $[Au(d2pype)_2]^+$ was observed (δ 26.0) but dynamic behaviour was evident in methanol. Variable temperature ^{31}P NMR data recorded in CH_3OH–CD_3OD solution are shown in Fig. 3. At 293 K, in addition to the $[Au(d2pype)_2]^+$ resonance at δ 26.8 a pair of multiplets is visible at δ 25.3 and 18.8. The latter peak is broadened but fine structure is clearly resolved for the multiplet at δ 25.3. The multiplets are assigned to the dimeric complex $[\{Au(d2pype)_2\}_2]^{2+}$ which has two distinct environments for chelated and bridging d2pype ligands.

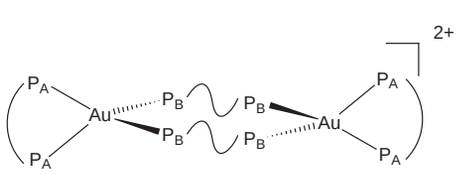

The ^{31}P COSY spectrum at 273 K (Fig. 4(a)) shows cross-peaks between the two multiplets confirming that they are part of the same spin-system. Although the broadening of the high field resonance precluded a complete analysis of the second order spin-system it is possible to assign the ^{31}P multiplet at δ 18.8 to the chelated (P_A) environment and the multiplet at δ 25.3 to the bridging (P_B) environment, based on the relative position of the multiplets and the splitting patterns which bear a strong resemblance to those observed in the ^{109}Ag-edited ^{31}P spectra of $[\{Ag(d2pype)_2\}_2]^{2+}$ where the assignment of P_A and P_B is unambiguous.[18] On cooling the solution in the temperature range 293–253 K the $[Au(d2pype)_2]^+$ resonance gradually decreased in intensity while the two multiplet resonances attributable to the dimer increased in intensity. The P_B multiplet remained sharp but the resonance attributed to the chelated P_A environment broadened slightly. The equilibrium between the monomer and dimer can be represented by:

$$[Au(d2pype)_2]^+ + [Au(d2pype)_2]^+ \rightleftharpoons [\{Au(d2pype)_2\}_2]^{2+} \quad (3)$$

with equilibrium constant $K_1 = [\{Au(d2pype)_2\}_2]/[Au(d2pype)_2]^2$. For the Ag(I) system we were able to obtain reliable estimates of K_1 by determining relative concentrations of monomer and dimer by by comparison of the ^{31}P peak integrals in the temperature range 298–213 K. However, this was precluded here since it is apparent from the ^1H NMR spectrum (Fig. 5a) that at temperatures below *ca.* 298 K the dimeric species is involved in an equilibrium with another species (*vide infra*).

At temperatures below *ca.* 253 K the P_B multiplet at δ 25.3 began to broaden and shifted to higher frequency so that at 203 K it had coalesced (at δ 26.0) with the $[Au(d2pype)_2]^+$ peak

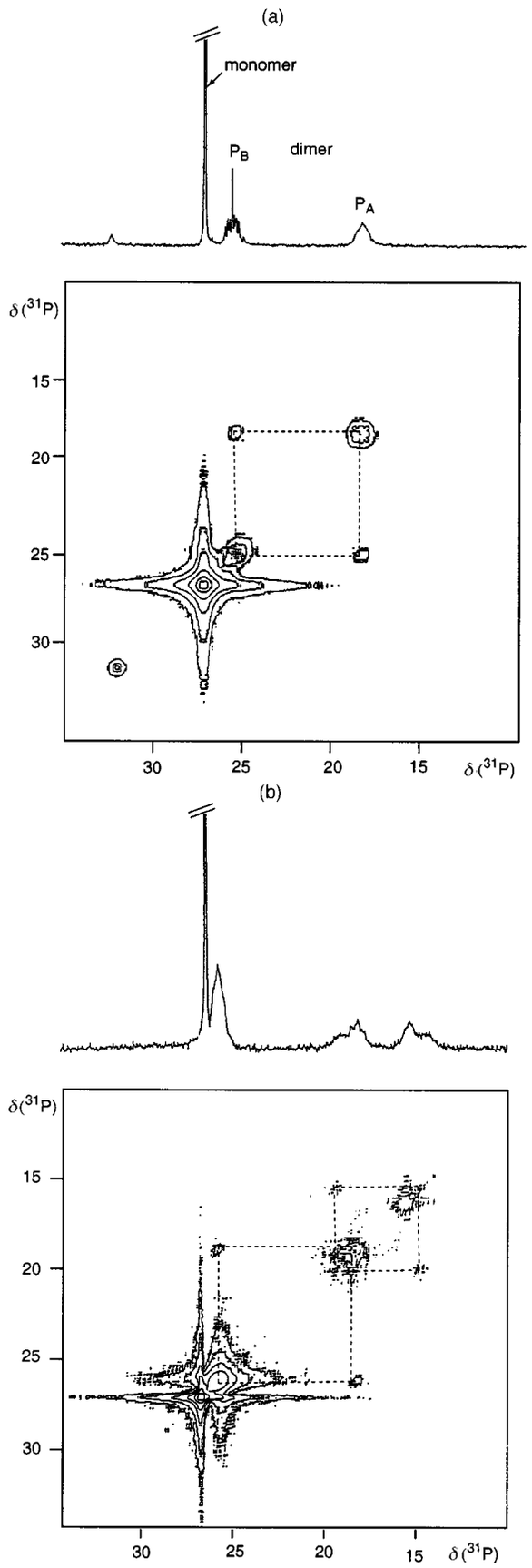

Fig. 4 Phase-sensitive $^{31}P\{^1H\}$ COSY spectra of the solution of $\{[Au(d2pype)_2]Cl\}_n$ in CH_3OH–30% CH_3OD at (a) 273 K and (b) 213 K with the $^{31}P\{^1H\}$ spectra shown as projections. The connectivities in (a) are between the P_A and P_B multiplets of the dimer, whereas in (b) although the connectivities between the P_A and P_B and P_B and P_C multiplets are consistent with both trimeric and tetrameric species, the relative intensities of the peaks are consistent with the tetrameric species (see text).

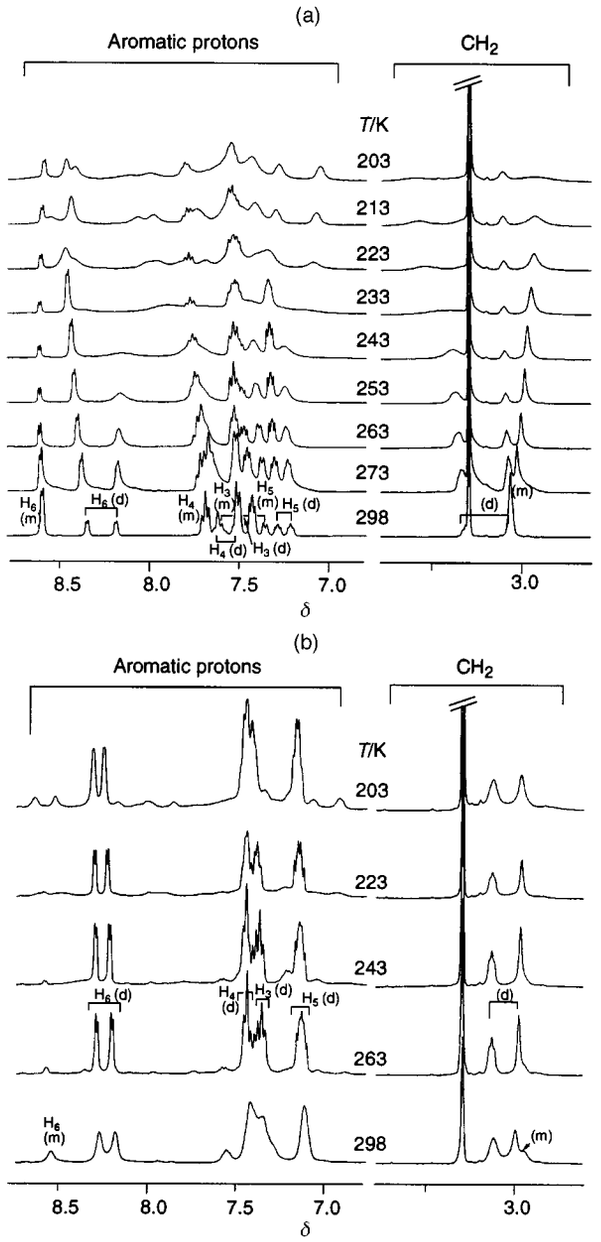

Fig. 5 ^1H spectra of (a) $\{[Au(d2pype)_2]Cl\}_n$ and (b) $\{[Ag(d2pype)_2]NO_3\}_n$ in CD_3OD at various temperatures, showing assignments for pyridyl and $P(CH_2)_2P$ protons in monomeric (m) and dimeric (d) species. For the Ag(I) system the additional peaks visible below 263 K are assignable to the trimeric cluster $\{[Ag(d2pype)_2]NO_3\}_3$ and the three species are in slow exchange on the NMR time scale.

which has a linear temperature dependence of 7.66×10^{-3} ppm K^{-1} (Fig. 3). The P_A multiplet peak continued to broaden on lowering the temperature and below 243 K split into two new broad peaks at δ 18.1 and 15.2 indicating the occurrence of further equilibria at low temperatures. In the temperature range 293–253 K the intensity of the monomer peak decreased from *ca.* 60 to 30% of the total Au–P species present, but it then remained relatively constant at temperatures between 253 and 223 K. This behaviour is clearly different from that observed for the analogous Ag(I) 2-pyridyl system, where peaks for both monomeric and dimeric species decreased in intensity on lowering the temperature and new peaks appeared due to a trimeric cluster. ^{31}P NMR resonances were resolved for all three species in the temperature range 263–213 K and they were in slow exchange on the NMR time scale.[18] In the present case there is evidence for the formation of a new species at low temperatures but the ^{31}P NMR spectra do not allow unambiguous assignment. A trimeric cluster $[\{Au(d2pype)_2\}_3]^{3+}$ has three non-

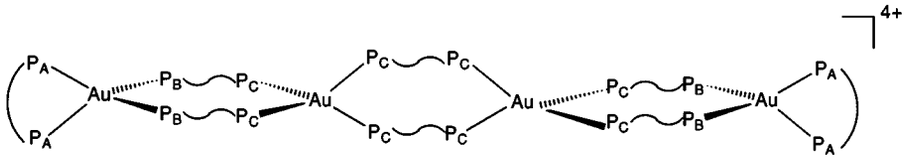

equivalent P sites corresponding to chelated (P_A) and bridging d2pype ligands coordinated to the terminal (P_B) and central (P_C) Au atoms, respectively. The ^{31}P COSY spectrum at 213 K (Fig. 4(b)) shows cross peaks between the central multiplet at δ 18.1 and both the other two multiplets at δ 15.3 and δ 25.1 indicating that the three P environments are within the same molecule. However, the relative intensity of the multiplet at δ 25.1 is approximately twice the intensity of the other two peaks whereas the trimeric cluster would contain P_A, P_B and P_C phosphorus sites in a ratio of 1 : 1 : 1. Since there is little change in the concentration of the monomer it is possible that the equilibrium at low temperatures corresponds to the formation of the tetrameric cluster from the dimer according to the following equation.

$$2[\{Au(d2pype)_2\}_2]^{2+} \rightleftharpoons [\{Au(d2pype)_2\}_4]^{4+} \quad (4)$$

The tetrameric cluster $[\{Au(d2pype)_2\}_4]^{4+}$ would also contain P_A, P_B and P_C phosphorus sites but in a ratio of 1 : 1 : 2, as is observed (see above).

However, the connectivities in the ^{31}P COSY spectrum are ambiguous as the peaks are very broad and there may be more than one species contributing to the central multiplet at δ 18.1. The possibility of aggregration to give the alternative tetrameric cluster, which has two non-equivalent P environments,

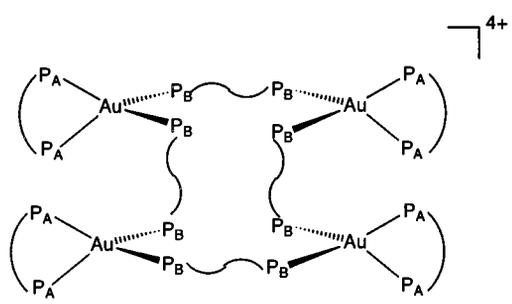

cannot be discounted. Since the ^{31}P spectra do not show peaks for both dimeric and tetrameric species in slow exchange it was not possible to confirm the assignment or to calculate the equilibrium constants for the reaction.

For the Ag system the dimeric complex was observed exclusively for a 10 mM solution of $\{[Ag(d2pype)_2]NO_3\}_2$ in acetonitrile at 295 K.[18] The ^{31}P NMR spectrum of a solution of $\{[Au(d2pype)_2]Cl\}_2$ in acetonitrile recorded under similar conditions (8.6 mM based on $[Au^+]$) showed the relative percentage of dimer (compared to monomer) to be only 35%. For a saturated solution of the complex in acetonitrile (*ca.* 26 mM based on $[Au]^+$) the relative percentage of dimer increased to a maximum of 55%.

The presence of an equilibrium mixture of the momeric and dimeric d2pype species in methanol was not apparent in ^{13}C NMR spectra, because separate peaks for monomer and dimer were not resolved (Table 2), but it was evident in the variable temperature ^{1}H NMR spectra of the system (Fig. 5(a)). In the aromatic region the H_6 proton of the pyridine ring of 2-pyridyl phosphines is strongly deshielded from the remaining aromatic protons[24] and occurs in a clear region of the spectrum. For the monomer the H_6 resonance is assignable to the peak at δ 8.60 since this decreased in intensity on cooling the solution, consistent with the behaviour observed in the ^{31}P NMR spectra. Similarly a pair of peaks of equal intensity at δ 8.17 and 8.34 can be assigned to the H_6 protons of pyridyl rings in the dimer in non-equivalent chelated and bridging d2pype ligands. By using these resonances as a reference point the other pyridyl ^{1}H resonances in the monomer and dimer were assigned from observed connectivities in phase-sensitive double-quantum filtered ^{1}H COSY spectra. These assignments are tabulated in Table 3. As observed for the ^{31}P spectra, the temperature dependent behaviour of the ^{1}H spectrum is significantly different from that observed for the analogous Ag(I) 2-pyridyl system. The variable temperature ^{1}H spectra of the Au(I) and Ag(I) complexes are compared in Fig. 5(a) and (b). For the Ag(I) system, the spectra show distinct resonances assignable to monomeric, dimeric and trimeric $\{[Ag(d2pype)_2]\}_n^{n+}$, and the three species are in slow exchange on the NMR time scale. For the Au(I) system the ^{1}H NMR spectrum at 298 K shows resonances for the monomer and dimer in slow exchange but as the solution is cooled the two peaks assigned to the H_6 protons of pyridyl rings in the dimer move apart. The peak at higher frequency remains relatively sharp at temperatures >243 K but the other peak broadens and disappears below 243 K. The H_6 resonance of the monomer decreases in intensity between 298 and 243 K, but then remains relatively constant. A similar pattern of behaviour is observed for the $P(CH_2)_2P$ bridge protons and is indicative of an equilibrium between the dimer and another species at an intermediate rate on the NMR time scale. An equilibrium between the dimer and tetrameric cluster (eqn. (4)) would be most likely. Also notable from comparison of the ^{1}H spectra is that for the Ag(I) dimer there is very little difference in chemical shift for protons in the chelated and bridging environments ($\Delta\delta$ 0.02–0.03), with the exception of H_6 ($\Delta\delta$ 0.09). On the other hand for the Au(I) system two distinct environments are observed for all four pyridyl protons ($\Delta\delta$ 0.07–0.24).

Structures

The differences between the solution state chemistry of the 2- and 4-pyridyl complexes are reflected also in the results obtained from the single crystal X-ray structure determinations. The 4-pyridyl complex was shown to crystallize as $[Au(d4pype)_2]Cl{\cdot}HCl{\cdot}6H_2O$ with the monomeric bis(chelated) cation, $[Au(d4pype)_2]^+$, two chloride and six water molecules constituting the asymmetric unit of the crystal lattice. The strong interactions between the 4-pyridyl substituents and the solvated water molecules lead to a well defined hydrogen-bond network between the water molecules, chloride anions and pyridyl nitrogens with N···O and O···O distances ranging from 2.5–2.9 Å and Cl···O and Cl···N distances from 3.0–3.2 Å. The chloride anion Cl(1) is located 3.0 Å from the pyridyl nitrogen N(12) and we postulate this nitrogen to be protonated such that the cation is better represented as $[Au(d4pype)_2H]^{2+}$ (*cf.* ref. 25). The Au–P bond lengths and P–Au–P bond angles in this complex correspond closely to those for the other monomeric bis(chelated) tetrahedral $[Au(P–P)_2]^+$ complexes reported, ranging from 2.36(1)–2.417(9) Å and 85.4(1)–137.5(3)° respectively (Table 4). Fig. 6 shows a view of the cation down the axis, approximately bisecting the bridging carbon atoms of the two ligands and passing through the gold atom (labelled '*z*' in Fig. 6). Each of the 4-pyridyl rings pairs with a ring on the other ligand, two along the '*y*' axis and two along the '*x*' axis of the cation, forming a cross-like structure. The two pairs of rings along $\pm y$ [(12), (42) and (22), (32)] lie in face-to-face mode with the distance between the rings *ca.* 3.5 Å. These rings participate strongly in the water/chloride/pyridyl

Table 4 AuP_4 geometric parameters (Å) for monomeric gold $[Au(P–P)_2]^+$ complexes

	dppe[a]	dppe[b]	dppey[c]	OH[d]	d4pype[e]
Au–P(1)	2.389(3)	2.412(2)	2.378(2)	2.368(1)	2.38(1)
Au–P(2)	2.416(3)	2.384(2)	2.388(2)	2.368(1)	2.36(1)
Au–P(3)	2.416(3)	2.402(2)	2.388(2)	2.354(2)	2.417(9)
Au–P(4)	2.392(3)	2.391(2)	2.377(2)	2.378(2)	2.376(9)
Au–P (avg.)	2.40(1)	2.40(1)	2.383(6)	2.37(1)	2.38(3)
P(1)–Au–P(2)	86.1(1)	87.1(1)	86.87(5)	86.44(4)	86.0(3)
P(1)–Au–P(3)	121.3(1)	113.1(1)	110.95(5)	123.21(4)	129.7(3)
P(1)–Au–P(4)	129.6(1)	117.2(1)	134.16(6)	120.78(4)	112.8(3)
P(2)–Au–P(3)	117.8(1)	124.8(1)	133.21(5)	123.21(4)	111.3(3)
P(2)–Au–P(4)	120.5(1)	130.6(1)	111.69(5)	102.78(4)	137.5(3)
P(3)–Au–P(4)	85.4(1)	86.4(1)	86.90(5)	86.66(6)	86.5(3)

[a] Ref. 22. [b] Ref. 26. [c] Ref. 27. [d] OH is $(HOH_2C)_2PC_6H_4P(CH_2OH)_2$, ref. 34. [e] This work.

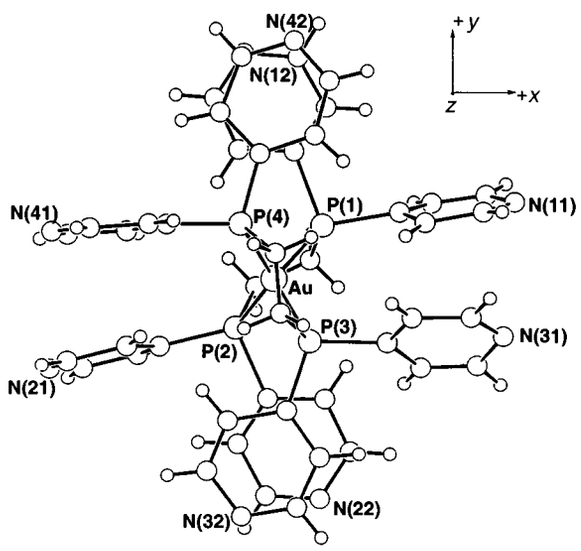

Fig. 6 Representative view of the $[Au(d4pype)_2]^+$ cation giving atom numbering. Atoms are shown as ideal spheres of arbitrary radius.

nitrogen hydrogen bonding network with, as noted above, N(12) likely to be protonated. The pairs of pyridyl rings along $\pm x$ [(11), (31) and (21), (41)] also lie parallel but are sheared away from each other and do not overlap. Comparison of the structure of this cation with that of $[Au(dppe)_2]^+$ [22,26] shows that for the latter the eight phenyl rings also interact in pairs with a similar cross-like disposition to those in the present cation, but which interact in both face-to-face and edge-to-face modes.

The dimeric structure of the 1:2 Au:d2pype adduct observed in solution is consistent with the crystallographic data which show the complex to crystallize as dimeric cations, $[(d2pype)Au(\mu\text{-}d2pype)_2Au(d2pype)]^{2+}$. In the present structure, obtained from methanol solution, 10 solvent/anion sites are identified, one of which is located on a two-fold axis. The electron densities of these sites were all similar and none could be definitively assigned as the chloride anions. All such sites were modelled as water which, after allowing for the two chlorides, leads to an estimate of 7 water molecules per Au atom. Unlike the structure of $[Au(d4pype)_2H]Cl_2{\cdot}6H_2O$ the location of the water/chloride anions in the lattice does not indicate any definite hydrogen-bonding interactions with the cation. A projection of the cation is shown in Fig. 7 with relevant geometric parameters listed in Table 5, together with comparative data for analogous dimeric copper and silver complexes. The two halves of the dimer are related by a crystallographic centre of symmetry with each gold atom coordinated to one bidentate and two bridging d2pype ligands with the bridging ligands and gold

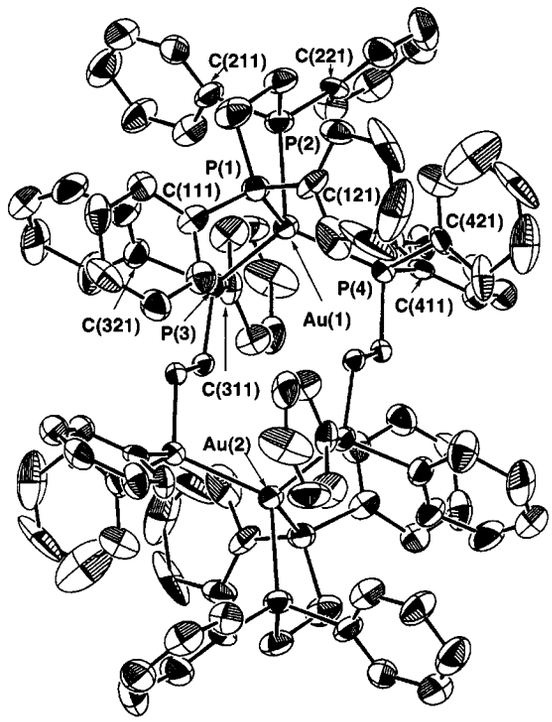

Fig. 7 Representative view of the $[Au(d2pype)_2]_2^{2+}$ cation giving atom numbering. Thermal ellipsoids are drawn at the 30% probability level. Hydrogen atoms have been omitted for clarity.

atoms forming a ten-membered ring in a double boat conformation. The core dimeric structure is similar to that for the analogous silver nitrate complex [18] with changes in the relative conformations of the pyridyl rings accommodating the changes in lattice structure, anion and co-crystallized solvent molecules. The Au–P bond lengths span a similar range (2.37–2.44 Å) to that found for the monomeric complexes with the bond lengths for the chelating ligand slightly longer than those for the bridging ligands while comparison with the data for dimeric copper and silver complex given in Table 5 shows the expected increase in the average M–P bond lengths in the order Cu < Au < Ag (*e.g.* ref. 27).

Attempts to obtain crystals of the monomeric complex from dimethylformamide (which was shown by the NMR studies to contain almost exclusively the monomeric complex) yielded only very small crystals. Partial solution of a very weak data set collected on one of these crystals [28] indicated that this complex also crystallizes as a dimeric rather than a monomeric complex.

Comparison with $[Au(dppe)_2]^+$

As found for the 1:2 complexes of $AgNO_3$ with bidentate pyridyl phosphines,[18] the 1:2 Au(I):d*n*pype complexes are more hydrophilic than the phenyl-substituted analogs and the degree of hydrophilicity depends critically on the position of the pyridyl N atom. The results of this study of the Au(I) chloride adduct and other crystallographic studies on 1:2 complexes of $AgNO_3$ [18] and copper iodide [29] with d2pype show that the dimeric $\{[M(d2pype)_2]^+\}_2$ structural type appears to be stabilized in the solid state with respect to the monomer by the d2pype ligand. For the Au(I) system our results show that even in solvents where the equilibrium strongly favours the monomeric form, the solubility properties of the dimer are such that this is the only species obtained in crystalline form. The 2-pyridyl complex has only limited solubility in water, and in this respect it is more similar to $[Au(dppe)_2]^+$ than the 3- and 4-pyridyl complexes. However, the 2-pyridyl system shows a strong tendency to aggregate as dimers, trimers or even tetramers depending on solvent and temperature; a result which suggests, as expected, greater interaction between solvent and

Table 5 MP_4 geometric parameters (Å) for dimeric $[(P–P)M(P\sim P)_2M(P–P)]^{2+}$ copper, silver and gold complexes

	Cu/dmpe[a]	Ag/d2pype[b]	Ag/dppe[c]	Ag/dmpe[d]	Au/d2pype[e]
M–P(1)	2.289(1)	2.50(1)	2.597	2.557(6)	2.416(6)
M–P(2)	2.293(1)	2.521(8)	2.509	2.491(4)	2.444(6)
M–P(3)	2.267(1)	2.46(1)	2.526	2.471(4)	2.378(6)
M–P(4)	2.263(1)	2.496(8)	2.550	2.465(4)	2.366(5)
M–P (avg.)	2.28(2)	2.49(3)	2.55(4)	2.50(4)	2.40(4)
P(1)–M–P(2)	89.2(1)	83.4(3)	84.1	83.5(2)	84.5(2)
P(1)–M–P(3)	116.9(1)	125.5(3)	118.0	114.1(2)	116.5(2)
P(1)–M–P(4)	113.2(1)	110.3(3)	119.4	144.4(2)	116.1(2)
P(2)–M–P(3)	110.3(1)	115.1(3)	118.5	115.6(2)	110.0(2)
P(2)–M–P(4)	115.1(1)	120.7(3)	106.4	117.6(2)	116.0(2)
P(3)–M–P(4)	110.7(1)	102.6(3)	108.4	109.6(2)	111.3(2)

[a] Ref. 35. [b] Ref. 18. [c] Ref. 36. [d] Ref. 37. [e] This work.

ligand than for dppe. By contrast the 3- and 4-pyridyl complexes are highly soluble in water, presumably a consequence of the more exposed N atoms. Interestingly, this results in the formation of monomeric complexes only. A comparison of the crystal structures of the monomeric tetrahedral cations $[Au(dppe)_2]^+$ and $[Au(d4pype)_2]^+$ shows that the change from phenyl to 4-pyridyl ligands does not change the nature of the AuP_4 core, or the overall structural topology of the cation, but there are major differences in the ways in which the substituents interact with the solvent which are consistent with the hydrophilic *versus* hydrophobic nature of the two ligands.

Relevance to antitumour activity

The results presented here are relevant to the interpretation of the differing antitumour activities of the Au(I) 2- and 4-pyridyl complexes in mice bearing i.p P388 leukaemia, which showed good activity for the 2-pyridyl complex but inactivity for the 4-pyridyl analogue.[5] These differences may be related, at least in part, to differences in their uptake into cells as a consequence of their different hydrophilic character. We have shown elsewhere[8] by ^{31}P NMR experiments that whereas the 2-pyridyl complex readily partitions between plasma and red blood cells, the water soluble 4-pyridyl complex is retained in the blood plasma fraction.

Our recent studies suggest that the antitumour properties of complexes related to $[Au(dppe)_2]^+$ are likely to be influenced by their stability and solubility properties and not necessarily by their three-dimensional structures, which we have shown here and elsewhere[18] to be versatile, with monomeric complexes able to exist in solution in equilibria with dimeric, trimeric and tetrameric species. An important factor is that all the active species are lipophilic cations (albeit with different hydrophilic–lipophilic character and charge), which are stable in solution and in the presence of thiols and blood plasma, with the aromatic substituents reducing the likelihood of oxidative side reactions in comparison to alkyl substituted phosphines.[5,6,8] An important difference between the pyridyl phosphine complexes, in comparison to $[Au(dppe)_2]^+$ and related antitumour complexes containing phenyl-substituents, is that the overall charge of the complexes (at physiological pH) will depend on the pK_a values of the pyridyl N atoms. The crystal structure of $[Au(d4pype)_2H]Cl_2\cdot 6H_2O$, which shows one of the 4-pyridyl nitrogens likely to be protonated, indicates that at least one 4-pyridyl nitrogen in the complex is highly basic and this has been confirmed by preliminary pK_a studies.[30]

Dppe and related diphosphine ligands exhibit antitumour activity[2] but are less potent (*ca.* 25-fold) than $[Au(dppe)_2]^+$ and in our earlier work[5,6] we speculated that the diphosphine was the active antitumour agent and coordination to the metal protects the ligand from unfavourable oxidation prior to delivery to intracellular target sites. A key feature in determining activity was thought to be the fine balance between the kinetic and thermodynamic stability of the M–P bonds since $[Au(dppe)_2]^+$ and other active Cu(I), Ag(I) and Au(I) diphosphine complexes possess enough kinetic lability in the M–P bonds to react *via* a ring-opening mechanism. Our recent work suggests that rather than the metal simply acting as a carrier for the active diphosphine ligand it may be the lipophilic cationic character of the complexes that is important for the antitumour activity. We noted previously[6] that for diphosphine ligands of the type $Ph_2P(CH_2)_nPPh_2$ antitumour activity is greatest for the ligands able to form 5- or 6-membered chelate rings (*i.e.* n = 2- or 3-, *cis*- but not *trans*-ethylene),[2] and proposed that the mechanism may involve chelation of metal ions. A further possibility is that the antitumour activity of the diphosphine ligands could be a consequence of the formation of lipophilic cationic complexes *in vivo* through metal complexation.

Several classes of lipophilic cations with anti-mitochondrial antitumour activity have demonstrated a relationship between antitumour selectivity and lipophilic balance[14,15] and our recent studies have shown a similar relationship for these gold(I) and related silver(I) pyridylphosphine complexes when tested against human ovarian cells in culture,[16,31] as well as differing toxicity to isolated rat hepatocytes.[31,32] We are currently investigating further the antitumour selectivity of these type of complexes and how these structural and other factors influence the lipophilicity, cellular uptake and cytotoxicity.

Acknowledgements

We acknowledge support of this work by the Australian Research Council, the Australian National Health & Medical Research Council and the Government Employees Medical Research Fund and thank Dr Peta Harvey for assistance with some of the NMR experiments and Mr Robbie Buckley and Mr Stephan Meier for assistance in the preparation of some of the compounds.

References

1 S. J. Berners-Price, C. K. Mirabelli, R. K. Johnson, M. R. Mattern, F. L. McCabe, L. F. Faucette, C.-M. Sung, S.-M. Mong, P. J. Sadler and S. T. Crooke, *Cancer Res.*, 1986, **46**, 5486.
2 C. K. Mirabelli, D. T. Hill, L. F. Faucette, F. L. McCabe, G. R. Girard, D. L. Bryan, B. M. Sutton, J. O. L. Bartus, S. T. Crooke and R. K. Johnson, *J. Med. Chem.*, 1987, **30**, 2181.
3 S. J. Berners-Price, R. K. Johnson, C. K. Mirabelli, L. F. Faucette, F. L. McCabe and P. J. Sadler, *Inorg. Chem.*, 1987, **26**, 3383.
4 S. J. Berners-Price, R. K. Johnson, A. J. Giovenella, L. F. Faucette, C. K. Mirabelli and P. J. Sadler, *J. Inorg. Biochem.*, 1988, **33**, 285.
5 S. J. Berners-Price, G. R. Girard, D. T. Hill, B. M. Sutton, P. S. Jarrett, L. F. Faucette, R. K. Johnson, C. K. Mirabelli and P. J. Sadler, *J. Med. Chem.*, 1990, **33**, 1386.
6 S. J. Berners-Price and P. J. Sadler, *Struct. Bonding* (*Berlin*), 1988, **70**, 27.
7 A. R. Khohkar, Q. Xu and Z. H. Siddik, *J. Inorg. Biochem.*, 1990, **39**, 117.

8 S. J. Berners-Price and P. J. Sadler, *Coord. Chem. Rev.*, 1996, **151**, 1.
9 Y. Dong, S. J. Berners-Price, D. R. Thorburn, T. Antalis, J. Dickinson, T. Hurst, L. Qui, S. K. Khoo and P. G. Parsons, *Biochem. Pharmacol.*, 1997, **53**, 1673.
10 S. J. Berners-Price, D. C. Collier, M. A. Mazid, P. J. Sadler, R. E. Sue and D. Wilkie, *Metal-Based Drugs*, 1995, **2**, 111.
11 G. F. Rush, D. W. Alberts, P. Meunier, K. Leffler and P. F. Smith, *Toxicologist*, 1987, **7**, 59.
12 P. F. Smith, G. D. Hoke, D. W. Alberts, P. J. Bugelski, S. Lupo, C. K. Mirabelli and G. F. Rush, *J. Pharmacol. Exp. Therap.*, 1989, **249**, 944.
13 G. D. Hoke, G. F. Rush, G. E. Bossard, J. V. McArdle, B. D. Jensen and C. K. Mirabelli, *J. Biol. Chem.*, 1988, **263**, 11203.
14 W. A. Denny, G. J. Atwell, B. C. Baguely and B. F. Cain, *J. Med. Chem.*, 1979, **22**, 134.
15 D. C. Rideout, T. Calogeropoulou, J. S. Jaworski, R. J. Dagino and M. R. McCarthy, *Anti-Cancer Drug Design*, 1989, **4**, 265.
16 S. J. Berners-Price, R. J. Bowen, M. J. McKeage, P. Galettis, L. Ding, C. Baguley and W. Brouwer, *J. Inorg. Biochem.*, 1997, **67**, 154.
17 R. J. Bowen, A. C. Garner, S. J. Berners-Price, I. D. Jenkins and R. E. Sue, *J. Organomet. Chem.*, 1998, **554**, 181.
18 S. J. Berners-Price, R. J. Bowen, P. J. Harvey, P. C. Healy and G. A. Koutsantonis, *J. Chem. Soc.*, *Dalton Trans.*, 1998, 1743.
19 R. W. Buckley, P. C. Healy and W. A. Loughlin, *Aust. J. Chem.*, 1997, **50**, 775.
20 TeXsan, Crystal Structure Analysis Package, Molecular Structure Corporation, 1992.
21 S. J. Berners-Price and P. J. Sadler, *Inorg. Chem.*, 1986, **25**, 3822.
22 S. J. Berners-Price, M. A. Mazid and P. J. Sadler, *J. Chem. Soc.*, *Dalton Trans.*, 1984, 969.
23 R. K. Harris, *Can. J. Chem.*, 1964, **42**, 2275.
24 G. E. Griffin and W. A. Thomas, *J. Chem. Soc. B*, 1970, 477.
25 Z. Assefa, B. G. McBurnett, R. J. Staples and J. P. J. Fackler, *Inorg. Chem.*, 1995, **34**, 75.
26 P. A. Bates and J. M. Waters, *Inorg. Chim. Acta*, 1984, **81**, 151.
27 S. J. Berners-Price, L. A. Colquhoun, P. C. Healy, K. A. Byriel and J. V. Hanna, *J. Chem. Soc.*, *Dalton Trans.*, 1992, 3357.
28 P. C. Healy, unpublished work.
29 S. J. Berners-Price, R. J. Bowen and P. C. Healy, unpublished work.
30 S. J. Berners-Price, R. W. Buckley, S. M. Dupen, L. R. Gahan and P. C. Healy, unpublished work.
31 S. J. Berners-Price, R. J. Bowen, P. Galettis, P. C. Healy and M. J. McKeage, *Coord. Chem. Rev.*, in the press.
32 M. J. McKeage, S. J. Berners-Price, L. Ding, P. Galettis, A. Farr, W. Brouwer and B. C. Baguley, *Proc. Am. Assoc. Cancer Res.*, 1998, **39**, 1506.
33 P. H. M. Budzelaar, J. H. G. Frijns and A. G. Orpen, *Organometallics*, 1990, **9**, 1222.
34 D. E. Berning, K. V. Katti, C. L. Barnes, W. A. Volkert and A. R. Ketring, *Inorg. Chem.*, 1997, **36**, 2765.
35 B. Mohr, E. E. Brooks, N. Rath and E. Deutsch, *Inorg. Chem.*, 1991, **30**, 4541.
36 H. Yang, L. Zheng, Y. Xu and Q. Zhang, *Wuji Huaxue Xuebao*, 1992, **8**, 65 (*Chem. Abstr.*, 1992, 117 212 593e).
37 V. Saboonchian, G. Wilkinson, B. Hussain-Bates and M. B. Hursthouse, *Polyhedron*, 1991, **10**, 737.

Paper 8/09285K